High sum-frequency generation in dielectric/antiferromagnet/Ag sandwich structures*

Fu Shu-Fang(付淑芳)[a)†], Liang Hong(梁 红)[b)c)], Zhou Sheng(周 胜)[a)], and Wang Xuan-Zhang(王选章)[a)]

[a)] *Key Laboratory for Photonic and Electronic Bandgap Materials, Ministry of Education, School of Physics and Electronic Engineering, Harbin Normal University, Harbin* 150025, *China*
[b)] *School of Electric Engineering, Harbin University of Science and Technology, Harbin* 150080, *China*
[c)] *School of Science, Harbin University, Harbin* 150086, *China*

(Received 15 August 2013; revised manuscript received 31 October 2013; published online 25 March 2014)

We present a method to increase the sum-frequency (SF) outputs in dielectric/antiferromagnet(AF)/Ag sandwich structures for a fixed input power. Two incident waves simultaneously illuminate the upper surface, one is oblique and the other is normal to it. Numerical calculations based on the $SiO_2/MnF_2/Ag$ and $ZnF_2/MnF_2/Ag$ structures show that the SF outputs on the upper film increase a few times as compared to those of a single AF film when the thickness of the AF film is one-quarter of the vacuum wavelength. Moreover, the SF outputs generated near the higher resonant frequency will be higher than those obtained near the lower resonant frequency. An optimum AF film thickness is achieved through investigating its effect on the SF outputs in the two different dielectric sandwich structures.

Keywords: sum-frequency generation, antiferromagnetic film, resonant frequency, nonlinear response

PACS: 75.50.Ee, 78.20.–e **DOI:** 10.1088/1674-1056/23/5/057503

1. Introduction

The sum-frequency (SF) generation technique has been widely used in the field of frequency conversion.[1–3] In the conversion process, light of two frequencies is mixed in a nonlinear crystal, resulting in the generation of new light sources at the sum or difference frequency. These three-wave mixing processes, also known as frequency upconversion or downconversion, are typically very sensitive to the incoming frequencies, due to the requirement of phase matching.[4,5] Actually, most materials, such as plasamas and semiconductors, are dispersive and absorbing. Thus, the film thickness, the strength of the incident light, or interaction mechanisms of two lights will affect the conversion efficiency of new light sources. An excellent review of four-wave mixing and phase conjugation in plasmas has been given by Federici.[6] Moore also performed theoretical and numerical analysis of resonant SF generation in an external cavity by varying the input coupler reflectivity. A scheme for generating a resonant SF in a semiconductor by employing a transverse wiggler magnetic field to it was presented.[7] The magnetic wiggler provides an uncompensated momentum required to make the process a resonant one.

In recent years, the nonlinearities of antiferromagnets (AFs) have been paid a great deal of attention, for example, the second-order harmonic generation and the optical bistability.[8–11] In addition, the resonant frequencies of typical AF materials are distributed over the far-infrared and millimeter ranges,[12–14] so their nonlinearity is of practical interest in these ranges. THz technology for future communication and detection applications could be possibly developed. However, a very strong electromagnetic wave is needed to illuminate the AF films in order to induce the nonlinearity of the AF films since the AF nonlinearity is weak. Almeida and Mills[15] and Kahn *et al.*[16] first discussed the bistable and multistable states of AF films and superlattices. According to their expectations, the magnetic component of the plane electromagnetic wave should reach a few tens of gauss, corresponding to the laser power of 100 MW/m^2, so a free-electron laser may be necessary. The SF outputs of a single AF film have been discussed, showing the continuous SF output windows versus the infrared signal wave frequencies.[17] However, the SF generation, a second-order nonlinear response of AF, is much weaker, leading to the lower SF conversion efficiency. Therefore, increasing the conversion efficiency at a fixed intensity is a very interesting subject. Zhou *et al.*[18,19] proposed a method to enhance the second-harmonic generation (SHG) by using an AF film for a fixed input power, in which the film is put between two different dielectrics or in one-dimensional photonic crystals. They raised the SH outputs to a few hundred times that of the single film. The method presented in this paper can be considered as an extension of their work. We propose a simple AF sandwich structure, dielectric/AF/Ag, in which Ag has a relatively higher dielectric constant and lower optical losses. If Ag is thick enough, the electromagnetic waves cannot penetrate it. The reflected electromagnetic waves will heighten the

*Project supported by the Young Academic Back-bone of Education Commission of Heilongjiang Province, China (Grant Nos. 1251G030 and12521154) and the National Natural Science Foundation of China (Grant Nos. 11104050, 11204056, and 11074061).

†Corresponding author. E-mail: shufangfu@yahoo.com

© 2014 Chinese Physical Society and IOP Publishing Ltd

field strength in the AF film. Thus, the SF outputs from the above film may be enhanced.

2. Theoretical model

As illustrated in Fig. 1, our attention is focused on the case where both the external magnetic field and AF anisotropy axis are along the z axis and parallel to layers. Two linearly polarized radiations are obliquely incident on the upper surface. I_l, R_l, and T_l indicate the incident, reflection and transmission waves, respectively, with the incident angle θ_l and transmission angle θ_l' ($l = 1$ or 2). $T_n^{\rm a}$ and $T_n^{\rm b}$ represent the corresponding output quantities of SF waves with direction angles θ_n and θ_n'. The two signal waves in the film are not indicated in Fig. 1. The dielectric function of the metal layers described by the Drude model is expressed by

$$\varepsilon_i(\omega_l) = 6 - \frac{\omega_{\rm p}^2}{\omega_l^2 - {\rm i}\rho\omega_l}, \tag{1}$$

where $\omega_{\rm p}$ is the resonant frequency of the metal and ρ is the damping.

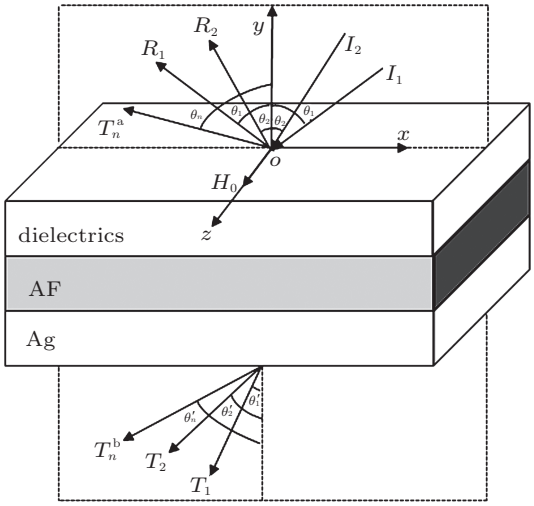


Fig. 1. Structures and Geometries: An AF film with the anisotropy axis normal to the incident plane is put between two different dielectrics. I_l, R_l, and T_l are the incident, reflective, and transmission waves with incident angle θ_l and transmission angle θ_l' ($l = 1$ or 2); $T_n^{\rm a}$ and $T_n^{\rm b}$ indicate the outputted SH waves with direction angles θ_n and θ_n'. The x–y plane is considered as the incident plane.

The SF magnetization arises as a source term in the SF wave equations and is excited by the pump waves, and in turn the pumping waves are induced by the incident waves. An assumption that the depletion of pump waves can be neglected is commonly accepted when the energy-flux density of the excited SF wave is much lower than those of the incident waves. Based on this assumption, solving the pump waves is a linear problem. Because the TM wave cannot excite the linear and SF magnetizations, we just take the TE wave with the electric field normal to the incident plane as the incident wave.[20] Therefore, the linear wave electric fields in various spaces can be describe as

$$E_{lz} = \exp({\rm i}k_{lx}x - {\rm i}\omega_l t) \times \begin{cases} I_{l0}\exp({\rm i}k_{l0}y) + R_{l0}\exp(-{\rm i}k_{l0}y), \\ \quad \text{in the above space}, \\ A_{lj}\exp({\rm i}k_{lj}y) + B_{lj}\exp(-{\rm i}k_{lj}y), \\ \quad \text{in the } j\text{-layer}, \\ T_{l0}\exp({\rm i}k_{l0}y), \\ \quad \text{in the below space}, \end{cases} \tag{2}$$

where the subscript $l = 1, 2$ describe the two pump waves, and $j = 1, 2$, a describe the dielectric and AFF layers, respectively. The wave-number components are

$$k_0 = [(\omega/c)^2 - k_{lx}^2]^{1/2}, \quad k_1 = [\varepsilon_1(\omega/c)^2 - k_{lx}^2]^{1/2},$$
$$k_2 = [\varepsilon_2(\omega/c)^2 - k_{lx}^2]^{1/2}, \quad k_{\rm a} = [\varepsilon_{\rm a}\mu_v(\omega/c)^2 - k_{lx}^2]^{1/2},$$

with $k_{lx} = (\omega/c)\sin\theta$, and the AF effective permeability $\mu_v = (\mu_{xx}^2 + \mu_{xy}^2)/\mu_{xx}$. The capital characters on the right-hand side of Eq. (2) represent the wave amplitudes in different spaces, where I_{l0}, R_{l0}, and T_{l0} are related to the incident, reflection, and transmission waves, respectively. In terms of ${\rm i}\omega\mu_0(1+\chi)\cdot\boldsymbol{H} = \boldsymbol{\nabla}\times\boldsymbol{E}$, the corresponding magnetic fields in different spaces are written as

$$H_{lx} = \frac{\exp({\rm i}k_{lx}x - {\rm i}\omega_l t)}{\omega_l\mu_0} \times \begin{cases} k_{l0}[I_{l0}\exp({\rm i}k_{l0}y) - R_{l0}\exp(-{\rm i}k_{l0}y)], \\ k_{lj}[A_{lj}\exp({\rm i}k_{lj}y) - B_{lj}\exp(-{\rm i}k_{lj}y)], \\ (k_{1{\rm a}}/\mu_v)[(1+\delta_l)A_{1{\rm a}}\exp({\rm i}k_{1{\rm a}}y) \\ \quad +(1-\delta_l)B_{1{\rm a}}\exp(-{\rm i}k_{1{\rm a}}y)], \\ k_{l0}T_{l0}\exp({\rm i}k_{l0}y), \end{cases} \tag{3}$$

where $\delta_l = {\rm i}k_{lx}\mu_{xy}(\omega_l)/\mu_{xx}(\omega_l)k_{l{\rm a}y}$. The y component of magnetic field in the AF film which will be used to calculate the second-order magnetization can be described as

$$H_{ly} = \frac{k_{lx}\exp({\rm i}k_{lx}x - {\rm i}\omega_l t)}{\omega_l\mu_0\mu_v}[(\delta_l' - 1)A_{1{\rm a}}\exp({\rm i}k_{1{\rm a}}y) - (\delta_l' + 1)B_{1{\rm a}}\exp(-{\rm i}k_{1{\rm a}}y)], \tag{4}$$

with $\delta_l' = {\rm i}\mu_{xy}(\omega_l)k_{1{\rm a}}/\mu_{xx}(\omega_l)k_{lx}$.

According to the boundary conditions, the matrix equation governing the reflection, transmission, and incident amplitudes can be derived as

$$\begin{pmatrix} I_{l0} \\ R_{l0} \end{pmatrix} = T_{t1}T_{1{\rm a}}T_{{\rm a}2}T_{2{\rm b}}\begin{pmatrix} T_{l0} \\ T_{l0} \end{pmatrix}. \tag{5}$$

Thus, the pumping amplitudes can be obtained by solving Eq. (5), which can be described as

$$\begin{pmatrix} I_{l0} \\ R_{l0} \end{pmatrix} = T_{t1}T_{1{\rm a}}\begin{pmatrix} A_{l{\rm a}} \\ B_{l{\rm a}} \end{pmatrix}, \tag{6}$$

where T in Eqs. (5) and (6) are the linear transfer matrixes as detailed in the Appendix A.

It is well known that SF waves are the second-order nonlinear response of AF film. In order to solve the output amplitudes of SF, the solution of the SF wave equation in the

AF film should be looked for. For TE waves, there is only one equation which contains a source term in the three components equations of the nonlinear wave equation. It is presented as

$$-\left(\frac{\partial^2}{\partial x^2}+\frac{\partial^2}{\partial y^2}\right)H_{nz}(\omega_n)-\varepsilon_{\rm a}(\omega_n/c)^2H_{nz}(\omega_n)$$
$$=\varepsilon_{\rm a}(\omega_n/c)^2\boldsymbol{m}_z^{(2)}(\omega_n). \tag{7}$$

The other two are homogenous and do not contain the field component $H_{nz}(\omega_n)$. It is evident that the SF wave is a TM wave since the other SF components cannot be excited without source terms. In the equation, $\boldsymbol{m}_z^{(2)}(\omega_n)$ is the second-order magnetization presented by

$$\begin{aligned}&\boldsymbol{m}_z^{(2)}(\omega_n)\\ &=\chi_{zxx}(H_{1x}(\omega_1)H_{2x}(\omega_2)+H_{1y}(\omega_1)H_{2y}(\omega_2))\\ &\quad+\chi_{zxy}(H_{1x}(\omega_1)H_{2y}(\omega_2)-H_{1y}(\omega_1)H_{2x}(\omega_2)),\end{aligned} \tag{8}$$

with $\omega_n=\omega_1+\omega_2$. The expressions of the second-order susceptibility can be found in the Appendix A. As an approximation, $\boldsymbol{H}_l(\omega_l)$ may be considered as the signal waves in the AF film induced by the incident waves.[21,22] Because the SF magnetization and pump field in the film both have been given, it is easy to find the solution of Eq. (7). Let

$$\begin{aligned}H_{nz}(\omega_n)&=[A_{na}\,{\rm e}^{{\rm i}k_{nay}y}+B_{na}\,{\rm e}^{-{\rm i}k_{nay}y}+N_1\,{\rm e}^{{\rm i}(k_{1ay}+k_{2ay})y}\\ &\quad+N_2\,{\rm e}^{-{\rm i}(k_{1ay}+k_{2ay})y}+N_3\,{\rm e}^{{\rm i}(k_{2ay}-k_{1ay})y}\\ &\quad+N_4\,{\rm e}^{-{\rm i}(k_{2ay}-k_{1ay})y}]\,{\rm e}^{({\rm i}k_{nx}x-{\rm i}\omega_n t)},\end{aligned} \tag{9}$$

where $k_{nay}=[\varepsilon_{\rm a}\mu_v(\omega_n/c)^2-k_{nx}^2]^{1/2}$ with $k_{nx}=k_{1x}+k_{2x}$. Substituting it into Eqs. (7) and (8), we find the nonlinear amplitudes

$$\begin{aligned}N_1&=\varepsilon_{\rm a}\omega_n^2F^+[\chi_{xzz}(\Delta_1^+\Delta_2^++\Delta_1'^-\Delta_2'^-)\\ &\quad+\chi_{zxy}(\Delta_1'^-\Delta_2^+-\Delta_1^+\Delta_2'^-)]A_{1a}A_{2a},\end{aligned} \tag{10a}$$
$$\begin{aligned}N_2&=\varepsilon_{\rm a}\omega_n^2F^+[\chi_{xzz}(\Delta_1^-\Delta_2^-+\Delta_1'^+\Delta_2'^+)\\ &\quad+\chi_{zxy}(\Delta_1^-\Delta_2'^+-\Delta_1'^+\Delta_2^-)]B_{1a}B_{2a},\end{aligned} \tag{10b}$$
$$\begin{aligned}N_3&=\varepsilon_{\rm a}\omega_n^2F^-[\chi_{xzz}(\Delta_1'^+\Delta_2'^--\Delta_1^-\Delta_2^+)\\ &\quad+\chi_{zxy}(\Delta_1^-\Delta_2'^-+\Delta_1'^+\Delta_2^+)]A_{2a}B_{1a},\end{aligned} \tag{10c}$$
$$\begin{aligned}N_4&=\varepsilon_{\rm a}\omega_n^2F^-[\chi_{xzz}(\Delta_1'^-\Delta_2'^+-\Delta_1^+\Delta_2^-)\\ &\quad-\chi_{zxy}(\Delta_1^+\Delta_2'^++\Delta_1'^-\Delta_2^-)]A_{1a}B_{2a},\end{aligned} \tag{10d}$$

where

$$F^\pm=\frac{1}{\omega_1\omega_2\mu_0^2\mu_{2v}(\omega_2)\mu_{1v}(\omega_1)\mu_1(\omega_2)\mu_1(\omega_1)\delta^\pm}, \tag{11a}$$
$$\delta^\pm=(k_{2a}\pm k_{1a})^2+(k_{1x}+k_{2x})^2-\varepsilon_{\rm a}\omega_n^2, \tag{11b}$$
$$\Delta_l^\pm=\mu_1(\omega_l)k_{lay}\pm{\rm i}\mu_2(\omega_l)k_{lx}, \tag{11c}$$
$$\Delta_l'^\pm=\mu_1(\omega_l)k_{lx}\pm{\rm i}\mu_2(\omega_l)k_{lay}. \tag{11d}$$

The solution (9) indicates that the SF wave in the film also propagates in the incident plane and will radiate out from the film. Therefore, we use $H_{nz}^{\rm a}=T_n^{\rm a}\,{\rm e}^{-{\rm i}k_{ny}y}\,{\rm e}^{({\rm i}k_{nx}x-{\rm i}\omega_n t)}$ to present the magnetic field of the SF wave generated above the film and $H_{nz}^{\rm b}=T_n^{\rm b}\,{\rm e}^{{\rm i}k_{ny}y}\,{\rm e}^{({\rm i}k_{nx}x-{\rm i}\omega_n t)}$ to indicate the SF field below, with k_{ny} determined by $k_{ny}^2+k_{nx}^2=\varepsilon_0(\omega_n/c)^2$. The SF electric fields in different spaces from $-{\rm i}\omega_n\varepsilon_0\varepsilon_{\rm a}\boldsymbol{E}_n=\boldsymbol{\nabla}\times\boldsymbol{H}_n$ are found to be

$$\boldsymbol{E}_n^{\rm a}=\frac{T_n^{\rm a}\,{\rm e}^{({\rm i}k_{nx}x-{\rm i}k_{ny}y-{\rm i}\omega_n t)}}{\omega_n\varepsilon_0\varepsilon_i}(k_{ny}\boldsymbol{e}_x+k_{nx}\boldsymbol{e}_y), \tag{12a}$$
$$\begin{aligned}\boldsymbol{E}_n&=-\frac{{\rm e}^{{\rm i}(k_{nx}x-\omega_n t)}}{\omega_n\varepsilon_0\varepsilon_{\rm a}}\{\boldsymbol{e}_x[k_{nay}(A_{na}\,{\rm e}^{{\rm i}k_{nay}y}-B_{na}\,{\rm e}^{-{\rm i}k_{nay}y})\\ &\quad+(k_{1ay}+k_{2ay})(N_1\,{\rm e}^{{\rm i}(k_{1ay}+k_{2ay})y}-N_2\,{\rm e}^{-{\rm i}(k_{1ay}+k_{2ay})y})\\ &\quad+(k_{2ay}-k_{1ay})(N_3\,{\rm e}^{{\rm i}(k_{2ay}-k_{1ay})y}-N_4\,{\rm e}^{-{\rm i}(k_{2ay}-k_{1ay})y})]\\ &\quad-\boldsymbol{e}_yk_{nx}(N_1\,{\rm e}^{{\rm i}(k_{1ay}+k_{2ay})y}+N_2\,{\rm e}^{-{\rm i}(k_{1ay}+k_{2ay})y}\\ &\quad+N_3\,{\rm e}^{{\rm i}(k_{2ay}-k_{1ay})y}+N_4\,{\rm e}^{-{\rm i}(k_{2ay}-k_{1ay})y})\},\end{aligned} \tag{12b}$$
$$\boldsymbol{E}_n^{\rm b}=\frac{T_n^{\rm b}\,{\rm e}^{({\rm i}k_{nyy}+{\rm i}k_{nx}x-i\omega_{sn}t)}}{\omega_n\varepsilon_0\varepsilon_i}(-k_{ny}\boldsymbol{e}_x+k_{nx}\boldsymbol{e}_y). \tag{12c}$$

Because the magnetic and electric fields are continuous at the interface, respectively, there must be $k_{nx}=k_{1x}+k_{2x}$. Then it is proven through the phase matching the propagation angles of the SF outputs from the film will not same with the propagation of linear reflective R_l and transmission T_l, respectively. One can get them from the relationship of the wave number in the different space. By a process similar to that described in the linear part, we can find the SF outputs. It is well known that the field components H_{sz} and E_{sx} are continuous at the interface between two adjacent media, thus, the magnetic amplitudes of the outputs R_n and T_n can be solved as follows:

$$\begin{pmatrix}0\\ T_n^{\rm a}\end{pmatrix}=M_{t1}[M_{1a}(M_{a2}M_{2b}\begin{pmatrix}T_n^{\rm b}\\ T_n^{\rm b}\end{pmatrix}+\Gamma_2)+\Gamma_1], \tag{13}$$

where the expressions of the nonlinear transfer matrix can be found in the Appendix A.

According to the definition, the incident electromagnetic energy-flux density in the nonmagnetic materials is written as $S_{Il}=(\varepsilon_0^2/\mu_0)^{1/2}|E_{0l}|^2/2$, but the SF output densities are expressed as $S_n^{\rm a}=(\mu_0/\varepsilon_0^2)^{1/2}|T_n^{\rm a}|^2/2$ for the above space of AFF and $S_n^{\rm b}=(\mu_0/\varepsilon_0^2)^{1/2}|T_n^{\rm b}|^2/2$ for its bottom space.

3. Numerical results and discussion

The numerical calculations are based on two examples, $SiO_2/MnF_2/Ag$ and $ZnF_2/MnF_2/Ag$, in which the AF film is MnF_2. The SF outputs depend on the field strength in the AF film, which are also relative to the reflection properties of the dielectric above or below the AF film in the sandwich structure. The thickness of Ag is chose as 8 μm where the order of the transmission of SF outputs are 10^{-7}. In this case, we assume that all the electromagnetic waves will be reflected into the AF film which will result in the increasing of the field strength in it. In order to study the influence of the dielectric constants on the SF outputs, we choose $\varepsilon_1=2.3$ or 8.0 for the SiO_2 or ZnF_2 layer which are respectively less or bigger than

$\varepsilon_a = 5.5$ for the AF film. The other physical parameters here applied are $M_0 = 0.6$ kG, $H_e = 550$ kG, $H_a = 7.87$ kG, and $\tau = 0.005$ for the MnF_2; the dielectric thickness will be fixed at $d_1 = 106$ μm which are a quarter of the vacuum wavelength of SiO_2; $\omega_p = 1.5 \times 10^{16}$ rad·s^{-1} and $\rho = 7.73 \times 10^{13}$ rad·s^{-1} for Ag. The external field , the resonant frequencies of MnF_2 are $\omega_{r1}/2\pi c = 9.76$ cm^{-1} and $\omega_{r2}/2\pi c = 9.83$ cm^{-1}. In order to compare with the results of a single AF film, the thickness of MnF_2 is also considered as one quarter of the wave length in the free space. In addition, the incident densities of the two signal waves are fixed at $S_{I1} = S_{I2} = 0.1$ MW/cm^2.

We first illustrate the output densities S_n^a and S_n^b of a single film versus the frequency ω_n and the incident angle θ_1 of the signal wave in Figs. 2 and 3 which are presented Ref. [15]. The other signal wave is normal to the surface of the film ($\theta_2 = 0°$) with the fixed frequencies $\omega_2 = 9.70$ cm^{-1} and 9.90 cm^{-1} which are near to the two resonant frequencies of AF film, respectively. The highest S_n^a and S_n^b have been marked with ω_n and θ_1 in the figures. Evidently, in terms of their respective maxima, S_n^b is stronger than S_n^a by one order for the two cases. Their maxima both are situated at the smaller incident angle regions in which most incident energy can participate in the course of SF generation.

The SF outputs of $SiO_2/MnF_2/Ag$ and $ZnF_2/MnF_2/Ag$ at $\omega_2 = 9.70$ cm^{-1} near the first resonant frequency are shown in Fig. 4. It is well known that the SF outputs cannot transmit into Ag if the thickness is thick enough. Therefore, the SF outputs S_n^b should be zero which are not presented here. Comparing the maxima of S_n^a with those of Fig. 2, we find that the

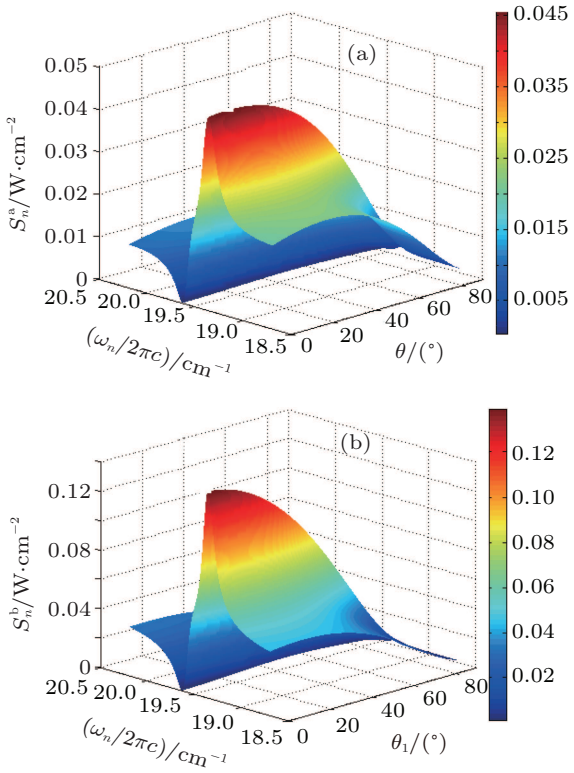


Fig. 2. (color online) SF outputs of a single film (MnF_2 film), (a) S_n^a and (b) S_n^b, versus the incident angle θ_1 and the SF frequency ω_n at $\omega_2 = 9.70$ cm^{-1} and $\theta_2 = 0$.

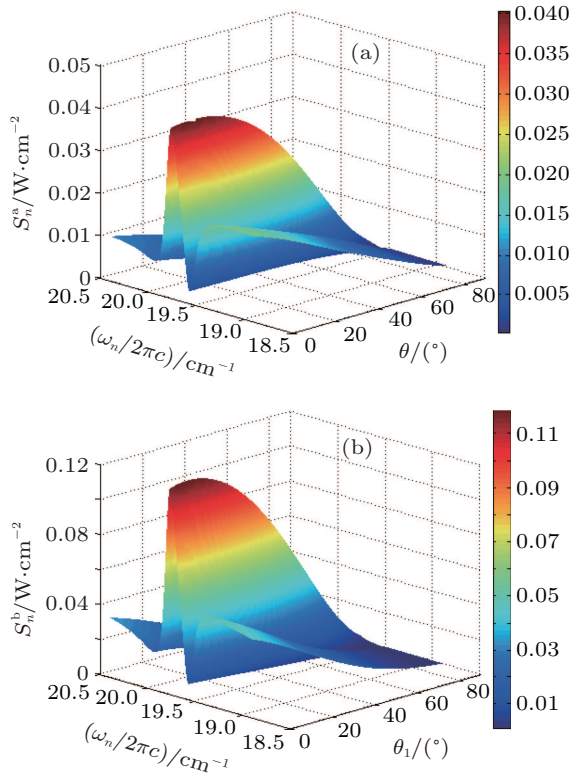


Fig. 3. (color online) SF outputs of a single film (MnF_2 film), (a) S_n^a and (b) S_n^b, versus the incident angle θ_1 and the SF frequency ω_n at $\omega_2 = 9.90$ cm^{-1} and $\theta_2 = 0$.

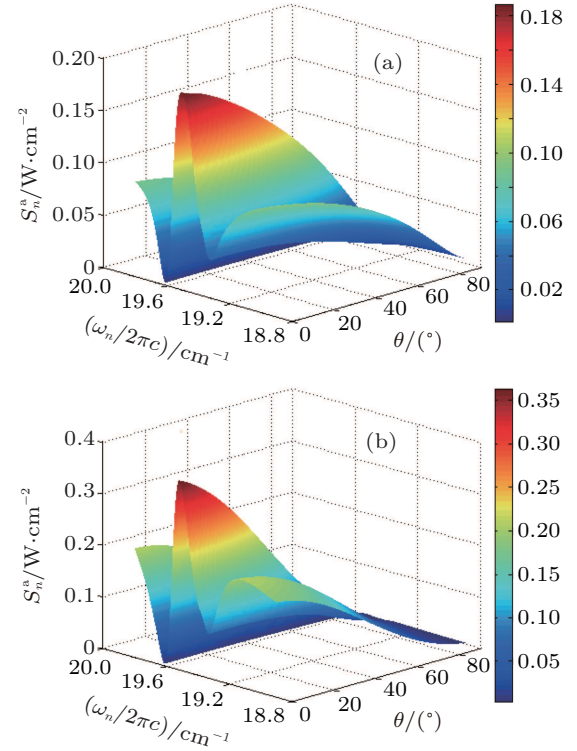


Fig. 4. (color online) SF outputs of $SiO_2/MnF_2/Ag$ and $ZnF_2/MnF_2/Ag$, S_n^a versus θ_1 and ω_n at $\omega_2 = 9.70$ cm^{-1} and $\theta_2 = 0$. (a) $x = 1.2$, $y = 19.51$, $z = 0.1873$; (b) $x = 0.3$, $y = 19.52$, $z = 0.3652$.

SF outputs of $SiO_2/MnF_2/Ag$ is about 4 times of reflection SF (RSF) outputs and 1.34 times of transmission SF (TSF) outputs of a single AF film. Also, S_n^a of $ZnF_2/MnF_2/Ag$ is about 8 and 2.6 times, respectively. It is apparent that the SF outputs of the sandwich structure $ZnF_2/MnF_2/Ag$ are almost 2 times of those generated from $SiO_2/MnF_2/Ag$.

Figure 5 shows that the SF outputs of the AF sandwich structures versus the incident angles and the SF frequency at $\omega_2 = 9.90$ cm^{-1} near the second resonant frequency. Compared with Fig. 3, the maxima of S_n^a is 6.95 times the RSF and 2.36 times the TSF of a single AF film for $SiO_2/MnF_2/Ag$, and also 15.78 and 5.36 times for $ZnF_2/MnF_2/Ag$. Also, the SF outputs of the SiO_2 sandwich structure are lower than those of the ZnF_2 sandwich structure. If we compare Figs. 4 and 5, it can be found that the SF outputs near the second resonant frequency will be higher than those obtained near the first resonant frequency.

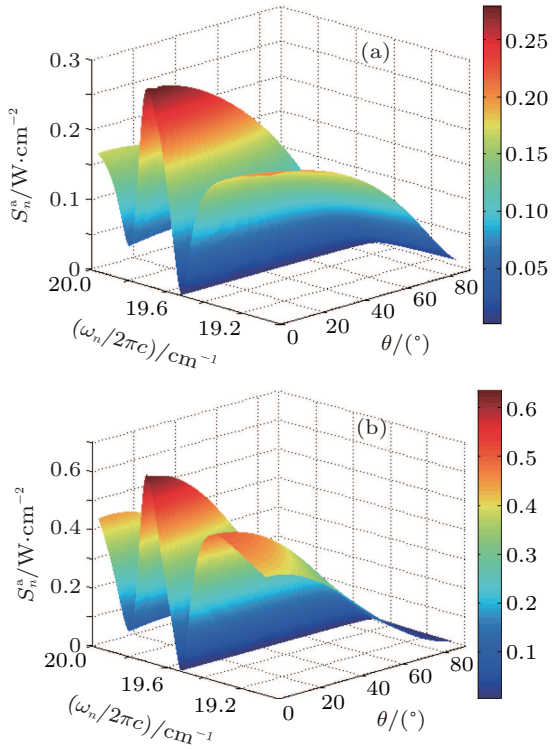


Fig. 5. (color online) SF outputs of $SiO_2/MnF_2/Ag$ and $ZnF_2/MnF_2/Ag$, S_n^a versus θ_1 and ω_n at $\omega_2 = 9.90$ cm^{-1} and $\theta_2 = 0$. (a) $x = 1.8$, $y = 19.71$, $z = 0.281$; (b) $x = 0.3$, $y = 19.71$, $z = 0.6383$.

The explanations for the enhanced SF outputs from the upper film are presented as follows. The signal waves in the film are composed of two parts, the forward and backward waves corresponding to the amplitudes A_l and B_l. The interference of the forward waves of the two signal waves will generate the SF and transmit from the bottom surface. The same interference course also occurs for the backward waves and the induced SF wave will propagate out from the upper surface. Since Ag cannot allow the electromagnetic wave to transmit through the SF outputs induced by the forward waves will almost be reflected back into the AF film, and interfere with the SF outputs waves induced by the backward pump wave, finally the enhanced SF outputs propagate out from the above surface when the phase difference between them satisfies $\varphi = \pm 2k\pi$ (k is an integer).

It is also interesting for us to examine SF outputs versus the AF film thickness in the two different dielectric sandwich structures. Figure 6 shows that S_n^a versus the thickness of AF when the incident frequency of the two signal pump waves are both near the second resonant frequency. The SF fringes are presented which maybe result from the change of optical thickness of the film. When AF is relatively thinner, the effect of the dielectric on the SF outputs will be obviously. However, when the thickness of AF becomes thicker, the SF outputs for the two sandwich structures are almost same. And an approximate saturation value is achieved at about $d = 510$ μm, $S_n^a = 3.85$ W·cm^{-2} which is nearly 95 and 32 times of S_n^a and S_n^b of the single AF film shown in Fig. 3. It can be expected that if we enhance the incident wave densities or focus it on a smaller area, a higher SF outputs are also obtained.

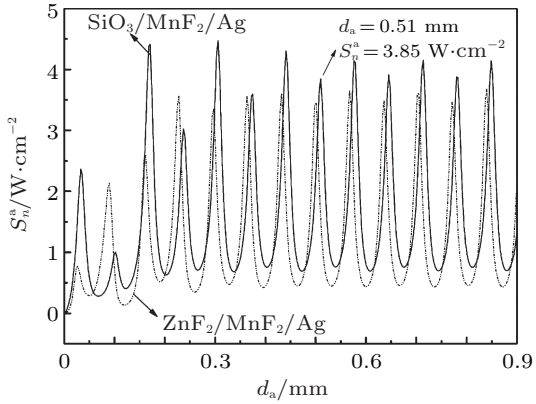


Fig. 6. SF outputs of $SiO_2/MnF_2/Ag$ and $ZnF_2/MnF_2/Ag$, S_n^a versus the optical thickness of AFF at $\omega_1 = 9.84$ cm^{-1}, $\omega_2 = 9.90$ cm^{-1}, and $\theta_1 = \theta_2 = 0$.

4. Conclusions

In this paper, we presented a method to increase the SF outputs of an AF film where a relative thick Ag layer is put below it. The numerical calculations are based on the $ZnF_2/MnF_2/Ag$ and $SiO_2/MnF_2/Ag$ structures. The SF outputs in the AF sandwich structure are a few times of a single AF film. In addition, the SF outputs of $ZnF_2/MnF_2/Ag$ are higher than those of $SiO_2/MnF_2/Ag$ when the thickness of AF film is one quarter of vacuum wavelength. In addition, the SF outputs near the higher resonant frequency are higher than those generated at the lower resonant frequency. The effect of the AF film thickness on the SF outputs is also investigated. An optimum AF film thickness is achieved where the effect of dielectric can be ignored and an approximate saturation value

of SF outputs for the two cases can be observed. The enhancement of SF generation will contribute to the preparation and application of the device in THz frequency field.

Appendix A

SF susceptibility

$$\begin{aligned}
&\chi^{(2)}_{zxx}(\omega_n)\\
&= \chi^{(2)}_{zyy}(\omega_n)\\
&= -\frac{1}{4M_0}[\chi^{(\prime 1)}_{xx}(\omega_1)n^{(\prime 1)}_{xx}(\omega_2)+n^{(\prime 1)}_{xx}(\omega_1)\chi^{(\prime 1)}_{xx}(\omega_2)\\
&\quad+\chi^{(1)}_{xy}(\omega_1)n^{(1)}_{xy}(\omega_2)+n^{(1)}_{xy}(\omega_1)\chi^{(1)}_{xy}(\omega_2)], \qquad \text{(A1a)}\\
&\chi^{(2)}_{zyx}(\omega_n)\\
&= -\chi^{(2)}_{zxy}(\omega_n)\\
&= -\frac{1}{4M_0}[\chi^{(1)}_{xy}(\omega_1)n^{(\prime 1)}_{xx}(\omega_2)+n^{(1)}_{xy}(\omega_1)\chi^{(\prime 1)}_{xx}(\omega_2)\\
&\quad-\chi^{(\prime 1)}_{xx}(\omega_1)n^{(1)}_{xy}(\omega_2)-n^{(\prime 1)}_{xx}(\omega_1)\chi^{(1)}_{xy}(\omega_2)], \qquad \text{(A1b)}
\end{aligned}$$

where

$$\begin{aligned}
\chi^{(1)}_{xx}(\omega) &= \chi^{(1)}_{yy}(\omega)\\
&= 2\omega_m\omega'_{\rm a}(\omega'^2_{\rm r}-\omega_0^2-\omega^2)/[\omega'^2_{\rm r}-(\omega-\omega_0)^2]\\
&\quad\times[\omega'^2_{\rm r}-(\omega+\omega_0)^2], \qquad \text{(A2a)}\\
\chi^{(1)}_{xy}(\omega) &= -\chi^{(1)}_{yx}(\omega)\\
&= -4{\rm i}\omega_m\omega'_{\rm a}\omega_0\omega/[\omega'^2_{\rm r}-(\omega-\omega_0)^2]\\
&\quad\times[\omega'^2_{\rm r}-(\omega+\omega_0)^2], \qquad \text{(A2b)}\\
n^{(1)}_{xx}(\omega) &= n^{(1)}_{yy}(\omega)\\
&= -2\omega_0\omega_m(\omega'^2_{\rm r}-\omega_0^2+\omega^2)/[\omega'^2_{\rm r}-(\omega-\omega_0)^2]\\
&\quad\times[\omega'^2_{\rm r}-(\omega+\omega_0)^2], \qquad \text{(A2c)}\\
n^{(1)}_{xy}(\omega) &= -n^{(1)}_{yx}(\omega)\\
&= 2{\rm i}\omega\omega_m(\omega'^2_{\rm r}+\omega_0^2-\omega^2)/[\omega'^2_{\rm r}-(\omega-\omega_0)^2]\\
&\quad\times[\omega'^2_{\rm r}-(\omega+\omega_0)^2]. \qquad \text{(A2d)}
\end{aligned}$$

Here $\omega'^2_{\rm r}=\omega'_{\rm a}(2\omega_{\rm e}+\omega'_{\rm a})$ with $\omega'_{\rm a}=\omega_{\rm a}+{\rm i}\tau\omega$. The other characteristic frequencies are $\omega_{\rm a}=\gamma H_{\rm a}$, $\omega_0=\gamma H_0$, $\omega_{\rm e}=\gamma H_{\rm e}$ and $\omega_m=4\pi\gamma M_0$, with γ being the gyromagnetic ratio. As the intermediate variable, $\boldsymbol{n}=\boldsymbol{m}_A-\boldsymbol{m}_B$ is defined here.

Linear transfer matrix The relation between the output above the film and the amplitudes in 1-layer is

$$\begin{pmatrix} I_0\\ R_0\end{pmatrix}=T_{t1}\begin{pmatrix} A_{l1}\\ B_{l1}\end{pmatrix}, \qquad \text{(A3a)}$$

with the matrix

$$T_{t1}=\frac{1}{2k_0}\begin{pmatrix} k_0+k_l & k_0-k_l\\ k_0-k_l & k_0+k_l\end{pmatrix}. \qquad \text{(A3b)}$$

The amplitudes in the 1-layer above and adjacent to the AF film and those in the AF film are conjoined by

$$\begin{pmatrix} A_{l1}\\ B_{l1}\end{pmatrix}=T_{1\rm a}\begin{pmatrix} A_{1\rm a}\\ B_{1\rm a}\end{pmatrix}, \qquad \text{(A4a)}$$

with the matrix

$$T_{1\rm a}=\frac{1}{2}\begin{pmatrix} (1+\delta^+_{l1})\exp(-{\rm i}k_{l1}d_1) & (1-\delta^-_{l1})\exp(-{\rm i}k_{l1}d_1)\\ (1-\delta^+_{l1})\exp({\rm i}k_{l1}d_1) & (1+\delta^-_{l1})\exp({\rm i}k_{l1}d_1)\end{pmatrix}, \qquad \text{(A4b)}$$

with $\delta^{\pm}_{l1}=(k_{1\rm a}\pm k_{lx}\mu_{xy}(\omega_l)/\mu_{xx}(\omega_l))/(\mu_v(\omega_l)k_{l1})$. The amplitudes in the AF film and those in the 2-layer below and adjacent to it are conjoined by

$$\begin{pmatrix} A_{l\rm a}\\ B_{l\rm a}\end{pmatrix}=T_{\rm a2}\begin{pmatrix} A_{l2}\\ B_{l2}\end{pmatrix}, \qquad \text{(A5a)}$$

where

$$T_{\rm a2}=\frac{\mu_v(\omega_l)k_{l2}}{2k_{1\rm a}}\begin{pmatrix} (\delta^-_{l2}+1)\exp(-{\rm i}k_{1\rm a}d_{\rm a}) & (\delta^-_{l2}-1)\exp(-{\rm i}k_{1\rm a}d_{\rm a})\\ (\delta^+_{l2}-1)\exp({\rm i}k_{1\rm a}d_{\rm a}) & (\delta^+_{l2}+1)\exp({\rm i}k_{1\rm a}d_{\rm a})\end{pmatrix}, \qquad \text{(A5b)}$$

where $\delta^{\pm}_{l2}=(k_{1\rm a}\pm k_{lx}\mu_{xy}(\omega_l)/\mu_{xx}(\omega_l))/(\mu_v(\omega_l)k_{l2})$. Finally, the relation between the amplitudes in the bottom layer and the transmission amplitude is

$$\begin{pmatrix} A_{l2}\\ B_{l2}\end{pmatrix}=T_{2\rm b}\begin{pmatrix} T_{l0}\\ T_{l0}\end{pmatrix}, \qquad \text{(A6a)}$$

with

$$T_{2\rm b}=\frac{1}{2k_{l2}}\begin{pmatrix} (k_{l2}+k_{l0})\exp(-{\rm i}k_{l2}d_2) & 0\\ 0 & (k_{l2}-k_{l0})\exp({\rm i}k_{l2}d_2)\end{pmatrix}. \qquad \text{(A6b)}$$

Nonlinear transfer matrix The matrix equation between the SF amplitudes in the AF film and the 1-layer above it is

$$\begin{pmatrix} A_{n1} \\ B_{n1} \end{pmatrix} = M_{1\mathrm{a}} \begin{pmatrix} A_{n\mathrm{a}} \\ B_{n\mathrm{a}} \end{pmatrix} + \Gamma_1, \tag{A7a}$$

where

$$M_{1\mathrm{a}} = \frac{1}{2k_{n1}\varepsilon_{\mathrm{a}}} \begin{pmatrix} (k_{n1}\varepsilon_{\mathrm{a}} - k_{n\mathrm{a}y}\varepsilon_1)\exp(-\mathrm{i}k_{n1}d_1) & (k_{n1}\varepsilon_{\mathrm{a}} + k_{n\mathrm{a}y}\varepsilon_1)\exp(-\mathrm{i}k_{n1}d_1) \\ (k_{n1}\varepsilon_{\mathrm{a}} + k_{n\mathrm{a}y}\varepsilon_1)\exp(\mathrm{i}k_{n1}d_1) & (k_{n1}\varepsilon_{\mathrm{a}} - k_{n\mathrm{a}y}\varepsilon_1)\exp(\mathrm{i}k_{n1}d_1) \end{pmatrix}, \tag{A7b}$$

and

$$\Gamma_1 = \frac{1}{2} \begin{pmatrix} [(1-\eta^+)N_1 + (1+\eta^+)N_2 + (1-\eta^-)N_3 + (1+\eta^-)N_4]\exp(-\mathrm{i}k_{n1}d_1) \\ [(1+\eta^+)N_1 + (1-\eta^+)N_2 + (1+\eta^-)N_3 + (1-\eta^-)N_4]\exp(\mathrm{i}k_{n1}d_1) \end{pmatrix}, \tag{A7c}$$

with $\eta^{\pm} = (k_{2\mathrm{a}y} \pm k_{1\mathrm{a}y})\varepsilon_1/k_{n1}\varepsilon_{\mathrm{a}}$. In addition, the relation between the SF amplitudes in the AF film and 2-layer below it is given by

$$\begin{pmatrix} A_{n\mathrm{a}} \\ B_{n\mathrm{a}} \end{pmatrix} = M_{\mathrm{a}2} \begin{pmatrix} A_{n2} \\ B_{n2} \end{pmatrix} + \Gamma_2, \tag{A8a}$$

where

$$M_{\mathrm{a}2} = \frac{1}{2k_{n\mathrm{a}y}\varepsilon_2} \begin{pmatrix} \mathrm{e}^{-\mathrm{i}k_{n\mathrm{a}y}d_{\mathrm{a}}}(k_{n\mathrm{a}y}\varepsilon_2 - \varepsilon_{\mathrm{a}}k_{n2}) & \mathrm{e}^{-\mathrm{i}k_{n\mathrm{a}y}d_{\mathrm{a}}}(k_{n\mathrm{a}y}\varepsilon_2 + \varepsilon_{\mathrm{a}}k_{n2}) \\ \mathrm{e}^{\mathrm{i}k_{n\mathrm{a}y}d_{\mathrm{a}}}(k_{n\mathrm{a}y}\varepsilon_2 + \varepsilon_{\mathrm{a}}k_{n2}) & \mathrm{e}^{\mathrm{i}k_{n\mathrm{a}y}d_{\mathrm{a}}}(k_{n\mathrm{a}y}\varepsilon_2 - \varepsilon_{\mathrm{a}}k_{n2}) \end{pmatrix}, \tag{A8b}$$

and

$$\Gamma_2 = \frac{1}{2} \begin{pmatrix} [-(1+\upsilon^+)\mathrm{e}^{\mathrm{i}(k_{1\mathrm{a}y}+k_{2\mathrm{a}y})d_{\mathrm{a}}}N_1 - (1-\upsilon^+)\mathrm{e}^{-\mathrm{i}(k_{1\mathrm{a}y}+k_{2\mathrm{a}y})d_{\mathrm{a}}}N_2 - (1+\upsilon^-)\mathrm{e}^{\mathrm{i}(k_{2\mathrm{a}y}-k_{1\mathrm{a}y})d_{\mathrm{a}}}N_3 - (1-\upsilon^-)\mathrm{e}^{-\mathrm{i}(k_{2\mathrm{a}y}-k_{1\mathrm{a}y})d_{\mathrm{a}}}N_4]\mathrm{e}^{-\mathrm{i}k_{n\mathrm{a}y}d_{\mathrm{a}}} \\ [-(1-\upsilon^+)\mathrm{e}^{\mathrm{i}(k_{1\mathrm{a}y}+k_{2\mathrm{a}y})d_{\mathrm{a}}}N_1 - (1+\upsilon^+)\mathrm{e}^{-\mathrm{i}(k_{1\mathrm{a}y}+k_{2\mathrm{a}y})d_{\mathrm{a}}}N_2 - (1-\upsilon^-)\mathrm{e}^{\mathrm{i}(k_{2\mathrm{a}y}-k_{1\mathrm{a}y})d_{\mathrm{a}}}N_3 - (1+\upsilon^-)\mathrm{e}^{-\mathrm{i}(k_{2\mathrm{a}y}-k_{1\mathrm{a}y})d_{\mathrm{a}}}N_4]\mathrm{e}^{\mathrm{i}k_{n\mathrm{a}y}d_{\mathrm{a}}} \end{pmatrix}, \tag{A8c}$$

with $\upsilon_1^{\pm} = (k_{2\mathrm{a}y} \pm k_{1\mathrm{a}y})/k_{n\mathrm{a}y}$. Other matrixes are given by

$$\begin{pmatrix} 0 \\ T_n^{\mathrm{a}} \end{pmatrix} = \frac{1}{2k_{n0}\varepsilon_1} \begin{pmatrix} k_{n0}\varepsilon_1 - k_{n1} & k_{n0}\varepsilon_1 + k_{n1} \\ k_{n0}\varepsilon_1 + k_{n1} & k_{n0}\varepsilon_1 - k_{n1} \end{pmatrix} \begin{pmatrix} A_{n1} \\ B_{n1} \end{pmatrix} = M_{t1} \begin{pmatrix} A_{n1} \\ B_{n1} \end{pmatrix}, \tag{A9}$$

$$\begin{pmatrix} A_{n2} \\ B_{n2} \end{pmatrix} = \frac{1}{2k_{n2}} \begin{pmatrix} (k_{n2} - \varepsilon_2 k_{n0})\exp(-\mathrm{i}k_{n2}d_2) & 0 \\ 0 & (k_{n2} + \varepsilon_2 k_{n0})\exp(\mathrm{i}k_{n2}d_2) \end{pmatrix} \begin{pmatrix} T_n^{\mathrm{b}} \\ T_n^{\mathrm{b}} \end{pmatrix} = M_{2\mathrm{b}} \begin{pmatrix} T_n^{\mathrm{b}} \\ T_n^{\mathrm{b}} \end{pmatrix}. \tag{A10}$$

References

[1] Mimoun E, Sarlo L D, Zondy J J, Dalibard J and Gerbier F 2008 *Opt. Express* **16** 18684
[2] Vance J D, She C Y and Moosmuller H 1998 *Appl. Opt.* **37** 4891
[3] Jeys T H, Brailove A A and Mooradian A 1989 *Appl. Opt.* **28** 2588
[4] Ji L L, Zhu B Q, Zhan T Y, Dai Y P, Zhu J, Ma W X and Lin Z Q 2011 *Acta Phys. Sin.* **60** 094210 (in Chinese)
[5] Zheng J J, Lu Y Q and Li P L 2010 *Acta Phys. Sin.* **59** 4687 (in Chinese)
[6] Federici J F 1991 *IEEE Trans. Plasma Sci.* **19** 549
[7] Moore G T 2002 *IEEE J. Quantum Electron.* **38** 12
[8] Fiebig M, Frohlich D, Krichevtsov B B and Pisarev R V 1994 *Phys. Rev. Lett.* **73** 2127
[9] Lim S C 2006 *J. Phys.: Condens. Matter* **18** 4329
[10] Fiebig M, Frohlich D, Lottermoser T, Pisarev R V and Weber H J 2001 *Phys. Rev. Lett.* **87** 137202
[11] Zhang Q, Zhou S, Li Q H and Fu S F 2012 *Acta Phys. Sin.* **61** 157501 (in Chinese)
[12] Abraha K and Tilley D R 1996 *Surf. Sci. Rep.* **24** 129
[13] Zhao Y, Fu S F, Li H and Wang X Z 2012 *IEEE Trans. Magn.* **48** 1597
[14] Sun D M, Fu S F, Zhou S and Wang X Z 2012 *J. Magn. Magn. Mater.* **324** 183
[15] Almeida N S and Mills D L 1987 *Phys. Rev. B* **36** 2015
[16] Kahn L, Almeida N S and Mills D L 1988 *Phys. Rev. B* **37** 8072
[17] Fu S F, Zhou S, Liang H and Wang X Z 2013 *J. Magn. Magn. Mater.* **346** 178
[18] Zhou S and Wang X Z 2008 *J. Opt. Soc. Am. B* **25** 1639
[19] Zhou S, Li H, Fu S F and Wang X Z 2009 *Phys. Rev. B* **80** 205409
[20] Boardman A D, Nikitov S A and Waby N A 1993 *Phys. Rev. B* **48** 13602
[21] Wang X Z and Fu S F 2004 *J. Magn. Magn. Mater* **271** 334
[22] Wang X Z and Li H 2005 *Phys. Rev. B* **72** 054403